Title

Spectral shifts of mammalian ultraviolet-sensitive pigments (short wavelength-sensitive opsin 1) are associated with eye length and photic niche evolution

Journal

Proceedings of the Royal Society B, 282(1819)

ISSN

0962-8452

Authors

Emerling, Christopher A
Huynh, Hieu T
Nguyen, Minh A
et al.

Publication Date

2015-11-22

DOI

10.1098/rspb.2015.1817

Peer reviewed

PROCEEDINGS B

rspb.royalsocietypublishing.org

Research

Cite this article: Emerling CA, Huynh HT, Nguyen MA, Meredith RW, Springer MS. 2015 Spectral shifts of mammalian ultraviolet-sensitive pigments (short wavelength-sensitive opsin 1) are associated with eye length and photic niche evolution. *Proc. R. Soc. B* **282**: 20151817.
http://dx.doi.org/10.1098/rspb.2015.1817

Received: 1 August 2015
Accepted: 9 October 2015

Subject Areas:
evolution, genetics

Keywords:
short wavelength-sensitive opsin 1, opsin, ultraviolet vision, colour vision, Mammalia

Authors for correspondence:
Christopher A. Emerling
e-mail: caemerling@berkeley.edu
Mark S. Springer
e-mail: mark.springer@ucr.edu

Electronic supplementary material is available at http://dx.doi.org/10.1098/rspb.2015.1817 or via http://rspb.royalsocietypublishing.org.

THE ROYAL SOCIETY
PUBLISHING

Spectral shifts of mammalian ultraviolet-sensitive pigments (short wavelength-sensitive opsin 1) are associated with eye length and photic niche evolution

Christopher A. Emerling[1,2], Hieu T. Huynh[1,3], Minh A. Nguyen[1,3], Robert W. Meredith[1,4] and Mark S. Springer[1]

[1]Department of Biology, University of California Riverside, Riverside, CA, USA
[2]Museum of Vertebrate Zoology, University of California Berkeley, Berkeley, CA, USA
[3]School of Pharmacy, Loma Linda University, Loma Linda, CA, USA
[4]Department of Biology and Molecular Biology, Montclair State University, Montclair, NJ, USA

Retinal opsin photopigments initiate mammalian vision when stimulated by light. Most mammals possess a short wavelength-sensitive opsin 1 (SWS1) pigment that is primarily sensitive to either ultraviolet or violet light, leading to variation in colour perception across species. Despite knowledge of both ultraviolet- and violet-sensitive SWS1 classes in mammals for 25 years, the adaptive significance of this variation has not been subjected to hypothesis testing, resulting in minimal understanding of the basis for mammalian SWS1 spectral tuning evolution. Here, we gathered data on SWS1 for 403 mammal species, including novel *SWS1* sequences for 97 species. Ancestral sequence reconstructions suggest that the most recent common ancestor of Theria possessed an ultraviolet SWS1 pigment, and that violet-sensitive pigments evolved at least 12 times in mammalian history. We also observed that ultraviolet pigments, previously considered to be a rarity, are common in mammals. We then used phylogenetic comparative methods to test the hypotheses that the evolution of violet-sensitive SWS1 is associated with increased light exposure, extended longevity and longer eye length. We discovered that diurnal mammals and species with longer eyes are more likely to have violet-sensitive pigments and less likely to possess UV-sensitive pigments. We hypothesize that (i) as mammals evolved larger body sizes, they evolved longer eyes, which limited transmittance of ultraviolet light to the retina due to an increase in Rayleigh scattering, and (ii) as mammals began to invade diurnal temporal niches, they evolved lenses with low UV transmittance to reduce chromatic aberration and/or photo-oxidative damage.

1. Introduction

Mammalian vision is initiated by the absorption of light by retinal photopigments, which are composed in part by the G-protein-coupled receptors known as opsins. The three visual opsins found in therian mammals—short wavelength-sensitive 1 (SWS1), long wavelength-sensitive (LWS) and rod opsin (RH1)—differ in their peak absorption wavelength (λ_{max}), with SWS1 ranging from ultraviolet-sensitive (350–370 nm; UVS) to violet-sensitive (400–457 nm; VS). UVS pigments are typically considered rare in mammals, having been directly measured in only 10 rodents [1–6] and four marsupials [7–9], although predictions based on SWS1 opsin sequences suggest that UVS pigments may be more widespread [8,10–20]. The utility of UVS versus VS pigments may be related to the detection of specific stimuli, particularly cues for foraging and communication [21–23]. Alternatively, broader selection pressures may govern the evolution of SWS1 spectral tuning. For example, UVS pigments would facilitate the detection of a wider spectrum of light than VS pigments, assuming a fixed λ_{max} for LWS [24]. Additionally, UVS SWS1 pigments may allow for greater chromatic contrast than VS SWS1

pigments due to increased spectral separation from LWS [25–27]. The widespread presence of UVS pigments in various vertebrates and the likelihood that a UVS SWS1 is the ancestral condition [28] suggests UVS pigments may be optimal for most vertebrate species. If correct, this raises the question of why most mammals have VS SWS1 pigments.

Prior to the discovery of UVS pigments in mammals by Jacobs *et al*. [1], Goldsmith [29] suggested that mammals lack UV receptors because their eyes have lenses that filter out ultraviolet light. Indeed, some diurnal mammal lenses transmit little to no UV light [30,31], but the lenses of certain nocturnal [18,30,31] and subterranean [4,20] mammals transmit UV light effectively, suggesting that photic niche (i.e. overall amount of light encountered by a species) may be influencing lens transmittance and ultimately SWS1 spectral tuning. Diurnal species may evolve lenses that reduce UV lens transmittance to limit the retina's exposure to damaging UV light and minimize chromatic aberration to improve visual acuity, though at the cost of reducing the wavelengths of light available to the retina and diminishing colour discrimination. This hypothesis predicts that species that occupy dim-light niches have UVS pigments, diurnal species have VS pigments and cathemeral/crepuscular mammals, which experience an intermediate amount of light, may have UVS or VS pigments. If UV-induced damage is a selection pressure driving lens evolution, then longevity may also influence SWS1 spectral tuning. Long-lived mammals experience greater amounts of UV light, on average, and therefore should have a higher likelihood of ocular damage than short-lived species. This hypothesis predicts that the ocular media of longer-lived mammals evolved to reduce retinal exposure to UV light. In fact, several mammals show a reduction in lens short-wavelength transmittance as they age [30,32], suggesting that longer-lived mammals are more likely to have VS pigments. A third hypothesis is that eye length influences SWS1 spectral tuning [33]. The ocular media as a whole (i.e. cornea, aqueous humour, lens, vitreous humour) can attenuate UV transmittance, probably due in part to increased Rayleigh scattering of shorter wavelengths. Longer eyes are predicted to increase UV scattering due to the longer optical path length, reducing the amount of UV light that reaches the retina, a hypothesis supported by an analysis of avian eyes [34]. The retention of UVS pigments in longer eyes would reduce the overall photon catch of SWS1 cones, therefore leading to selection for VS pigments.

Here we test whether increases in photic niche brightness, longevity and eye length lead to increased SWS1 λ_{max}. We predict that the evolution of SWS1 spectral sensitivity in mammals is directly driven by the evolution of the ocular media, which in turn is influenced by the evolution of photic niche, longevity and eye length. Our results suggest that the ancestral therian mammal possessed a UVS SWS1, and this shifted to VS on at least 12 occasions in association with increases in light exposure and eye length.

2. Material and methods

We collected data on the presence/absence of SWS1 cones and spectral tuning of SWS1 opsin from the literature, GenBank, *in silico* assemblies of *SWS1* from publicly available genomes (Ensembl; PreEnsembl; NCBI's whole genome shotgun database, hereafter WGS), and *de novo* sequences of *SWS1* exon 1 generated from PCR amplification (electronic supplementary material, table S1). We deemed SWS1 cones as present in a species under the following conditions: positive immunostaining of cones with SWS1 opsin antibodies, electrophysiological or microspectrophotometric recordings of the retina/individual cones with a λ_{max} consistent with SWS1 (approx. 350–450 nm), *SWS1* mRNA expression in retinal extracts, and/or the presence of intact *SWS1* DNA sequences that lack inactivating mutations. Though none of the methods individually provides proof positive of functional SWS1 cones, there is a high level of consonance between the methods, suggesting that this is a reliable approach (see references in the electronic supplementary material, table S1). We concluded that SWS1 cones are absent when there were negative results from any of the above methods. When more than one λ_{max} estimate was reported in the literature, we selected the largest value for phylogenetic generalized least-squares (PGLS) analyses. We assembled sequences from genomes after BLASTing query mRNA sequences from GenBank against the genome databases using the BLAT algorithm for Ensembl/PreEnsembl and discontiguous megablast for WGS. If we had negative results, we used a less restrictive BLAST algorithm and/or query sequences from more closely related species. For *de novo* sequences, we designed primers based on the 5′ UTR and intron 1 of *SWS1* genome sequences of closely related taxa (electronic supplementary material, table S2). We performed nested PCR with Ramp-Taq DNA polymerase (Denville Scientific Inc.) in 50 ml reactions with the following thermal cycling parameters: template denaturation at 95°C for 7 min; 45 cycles of 1 min at 95°C (denaturation), 1 min at 50°C (annealing) and 2 min at 72°C (extension); a final extension at 72°C for 10 min. We used 500–750 ng of genomic DNA for the initial PCR reactions and 1–1.5 ml of PCR product in the nested PCR reactions. We assayed the final PCR products on 1% agarose gels, excised bands of interest with razor blades, and cleaned them with the Bioneer AccuPrep Gel Purification kit. Purified PCR products were sequenced in both directions at the UCR Core Instrumentation Facility with an automated DNA sequencer (ABI 3730xl). We performed contig assembly in Geneious [35] v. 5.6.5 using the Muscle alignment tool [36]. All sequences were aligned manually with Se-Al v. 2.0a11 [37].

We collected data for eye length (i.e. axial diameter) from various sources (electronic supplementary material, table S3), longevity from PanTHERIA [38] and AnAge [39], and photic niche from PanTHERIA and the literature (Hall *et al*. [40] and Roll *et al*. [41], and mammalian species accounts as listed in electronic supplementary material, table S3). In cases where eye length or longevity data conflicted, we selected the largest value reported among the sources. We coded photic niche as mesopic (*sensu* Jones *et al*. [38]) when data conflicted.

We performed ancestral DNA sequence reconstructions of *SWS1* using 218 mammals and eight outgroup taxa (electronic supplementary material, dataset S1) to infer historical shifts in spectral tuning based on residues 86 and 93 + 114 (see below; bovine RH1 numbering here and throughout). We used both putatively functional and pseudogenic sequences to increase taxonomic coverage. We performed reconstructions with codeml in PAML v. 4.4 [42], and compared four codon frequency models using the Akaike information criterion, with equal codon frequencies providing the best fit (electronic supplementary material, table S4).

We predicted the spectral tuning for newly reported sequences (genome- and PCR-derived) on the basis of comparative sequence and mutagenesis data (electronic supplementary material, tables S1 and S5). We recorded 13 residues in exon 1 of *SWS1* known to affect spectral tuning [43]. All examined mammalian SWS1 sequences with F86 and T93 have UVS pigments, whereas possessing a tyrosine, serine or valine at 86 yields a VS pigment. By contrast, primates have a unique sequence combination that produces a VS pigment, apparently being determined by possessing a P93 (electronic supplementary material, table S1). Mutagenesis studies have demonstrated the importance of these amino acids in shifting UVS to VS pigments and vice versa [44–52], whereas

mutations at other sites only induce minor spectral shifts. Therefore, we predicted that an SWS1 pigment is UVS if it possesses F86 and T93, and a VS pigment if it has Y86, S86, V86 or P93.

We estimated a phylogeny for mammalian species with data for SWS1 cones (i.e. presence/absence and/or spectral tuning), and added mammalian species and tetrapod outgroups from Meredith *et al*. [53] to provide a robust backbone for the tree. We only included one representative from each cetacean family due to the parallel inactivation of *SWS1* in odontocetes and mysticetes [54]. Some taxa with high percentages of missing gene sequences and/or non-overlapping sequences (e.g. with other congeners) resisted robust phylogenetic placement and were not included in phylogenetic analyses. Finally, we added species to minimize long-branch misplacement (e.g. *Miniopterus* spp.). We collected DNA sequences for 38 genes (27 nuclear and 11 mitochondrial) from GenBank and various genomic resources (electronic supplementary material, table S6, dataset S2). We used the discontiguous megablast algorithm to obtain GenBank and WGS sequences, and BLAT for Ensembl and PreEnsembl sequences. We aligned sequences with MUSCLE in GENEIOUS and adjusted them manually in SE-AL. Alignment-ambiguous regions and contaminants were excluded prior to phylogenetic analysis. We concatenated the final gene alignments into a DNA supermatrix with SEQUENCEMATRIX [55] v. 1.7.8, and executed a RAxML [56] (v. 8.1.11) analysis on CIPRES [57], giving each gene partition its own model of DNA sequence evolution (GTRGAMMA). We ran 500 bootstrap iterations with GTRCAT but otherwise used the default settings on CIPRES.

We estimated divergence times with chronos in the APE package in R [58–60]. We estimated the smoothing parameter with the cross-validation method implemented in chronopl in APE, starting at 0 and using a logarithmic scale from 10^{-6} to 10^{14}. We set the smoothing parameter to the optimal value (10^{7}), employed 77 calibrations (electronic supplementary material, calibrations) and used the correlated model of sequence evolution. We implemented the resulting timetree in all subsequent phylogenetic comparative analyses.

We tested the hypothesis that the average amount of light exposed to the eye (photic niche) is correlated with spectral tuning with SIMMAP v. 1.5 [61,62]. We coded photic niche as scotopic/dim light (0) for nocturnal and subterranean species, mesopic/moderate light (1) for cathemeral and crepuscular species, or photopic/bright light (2) for diurnal species. We coded spectral tuning as UVS (0) or VS (1) based on measured λ_{max} and/or DNA sequence predictions. We estimated character evolution priors [63] using the MCMC method described in SIMMAP (cycles: 100 000; sampling freq: 200; burnin: 10 000; rate upper bound: 1000): (i) photic niche: rate prior parameter $\alpha = 26.128$, $\beta = 2006.996$; (ii) spectral tuning: rate prior parameter $\alpha = 8.870$, $\beta = 3616.625$, bias parameter $\alpha = 85.737$. We set the bias parameter for photic niche to empirical, and used the default number of categories (k) for the priors (bias = 31; rate = 60). We pruned all species from the timetree that lacked sufficient data, and ran analyses with state ordering for photic niche as unordered and ordered. Sampling settings for the correlation analysis were 2000 samples, 10 prior draws and 1000 predictive samples.

We used phylogenetic logistic regression [64] to test the hypotheses that longevity and eye length predict spectral tuning, respectively. We coded spectral tuning as above, and log-transformed longevity and eye length prior to analysis. After pruning taxa with insufficient data, we converted the reduced timetrees into variance–covariance matrices (vcv function in APE). We performed phylogenetic logistic regression using the PLogReg function in MATLAB [65] with 2000 bootstrap simulations to calculate confidence intervals. We standardized the independent variables to have a mean of zero and a variance of one, and set the initial estimate of a to -1.

We performed PGLS [66] in the caper package in R [67] to test the hypotheses that photic niche, longevity and eye length influence SWS1 λ_{max} individually and in concert. We coded the independent variables as above, and pruned all species from the timetree that lacked data on λ_{max} and at least one of the predictor variables. We used a phylogenetic correction based on a maximum-likelihood estimate of Pagel's λ, which in each case equalled 1.

3. Results and discussion

We assembled 40 complete or partial *SWS1* sequences derived from published genomes, and generated 57 complete or partial *SWS1* exon 1 sequences via PCR and Sanger sequencing for a total of 97 novel sequences (electronic supplementary material, dataset S3). Five novel sequences are pseudogenes (electronic supplementary material, table S7), suggesting that these species lack SWS1 cones. Three species—*Odobenus rosmarus* (walrus), *Callorhinus ursinus* (northern fur seal), *Notoryctes typhlops* (marsupial mole)—have intact coding sequences for complete or partial *SWS1*, but external evidence suggests that SWS1 cones are absent in each [68–70]. Our combined dataset describes 270 species with functional SWS1 cones, 214 of which have measured or predicted spectral tuning (electronic supplementary material, table S1), and 133 with non-functional SWS1 cones, a common trait in species occupying scotopic niches (see [2,12,17,49,54,69–71] for discussion). Our novel sequence data increase the taxonomic coverage of SWS1 spectral tuning to 39 additional mammalian families. In total, we report 89 species with UVS pigments and 125 with VS pigments. These proportions suggest that UVS pigments in mammals are far more prevalent (41.6%) than previously assumed, which becomes even more apparent considering that the most diverse mammalian clades (e.g. murid and cricetid rodents, bats) so far only appear to possess UVS pigments.

We performed ancestral sequence reconstructions to infer the history of SWS1 spectral tuning in mammals. The topology we used (RAxML best tree) can be found in the electronic supplementary material (dataset S4). Based on changes in key residues, our reconstructions indicate that therian mammals inherited a UVS SWS1 pigment from an amniote ancestor, which shifted to a VS pigment on at least 12 occasions (figure 1). Seven shifts to a VS pigment occurred via F86Y, two through F86V, one by F86S, and on the stem Primates branch, a T93P substitution was accompanied by A114G (electronic supplementary material, table S8). Though Carvalho *et al*. [52] showed that introducing a P93T mutation into the aye-aye (*Daubentonia madagascariensis*) VS SWS1 pigment shifts it to UVS, Shi *et al*. [51] demonstrated that T93P is not sufficient to induce a mouse (*Mus musculus*) UVS pigment to shift to VS. Upon closer inspection, we found that the aye-aye and ancestral primate pigments are identical to the mouse UVS pigment at every tuning site except P93 and G114. Shi *et al*. [51] created four mouse SWS1 mutants that had P93 + G114, all of which shifted mouse UVS to VS. Together these data suggest that the shift of primate pigments from UVS to VS is accomplished by T93P + A114G as opposed to T93P alone. Most examined primate SWS1 pigments retain P93 + G114, with cercopithecids and *Cebus* reverting to A114, and presbytins acquiring S114. However, these latter species possess additional substitutions that appear to have allowed them to retain VS pigments in the absence of G114 (electronic supplementary

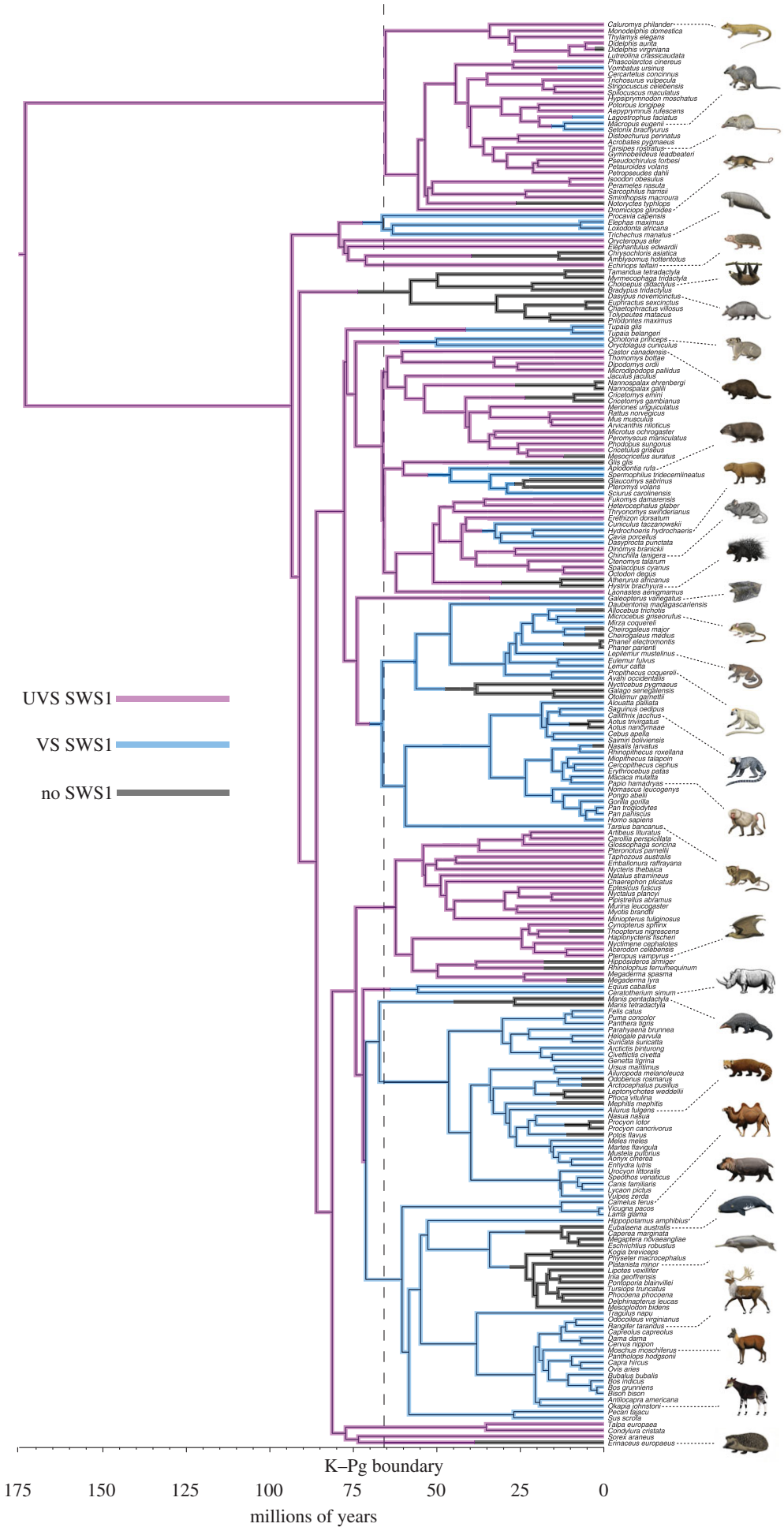

Figure 1. (*Caption overleaf.*)

Figure 1. (*Overleaf*.) Timetree with collapsed branches showing the diversity and major evolutionary transitions of SWS1 in mammals. Changes in colour along branches represent SWS1 transitions and have been arbitrarily dated to the midpoint of the branch on which they occurred. For species for which no sequence data are available, we indicated their most parsimonious ancestral states. For species that have complete *SWS1* pseudogene sequences but show no evidence of shared inactivating mutations with other species, we assumed they lost SWS1 independently (e.g. pinnipeds). Paintings by Carl Buell, copyright John Gatesy.

Table 1. Results from SiMMAP analyses. M and D represent the overall correlation between traits, and m and d indicate state-by-state correlations. For state-by-state correlations: before comma = photic niche (Sc = scotopic; Me = mesopic; Ph = photopic); after comma = spectral tuning. Positive value = positive association between states; negative value = negative association. Bold *p*-values are <0.05.

	unordered		ordered	
statistic	value	*p*-value	value	*p*-value
M	0.095164	**0.015**	0.130264	**0.013**
m(Sc,UVS)	0.112146	**0.006**	0.132556	**0.003**
m(Sc,VS)	−0.076043	**0.002**	−0.079747	**0.001**
m(Me,UVS)	−0.030418	0.062	−0.039905	**0.004**
m(Me,VS)	0.043092	0.071	0.055572	**0.01**
m(Ph,UVS)	−0.028834	**0.04**	−0.019639	0.08
m(Ph,VS)	0.07522	**0.009**	0.081426	**0.015**
D	0.385206	**0.009**	0.440227	**0.004**
d(Sc,UVS)	0.096194	**0.003**	0.110043	**0.001**
d(Sc,VS)	−0.096198	**0.003**	−0.110047	**0.001**
d(Me,UVS)	−0.037621	0.068	−0.048824	**0.008**
d(Me,VS)	0.037619	0.068	0.048821	**0.008**
d(Ph,UVS)	−0.058577	**0.014**	−0.061223	**0.022**
d(Ph,VS)	0.058575	**0.014**	0.061222	**0.022**

material, table S1). Three tuning site substitutions on the stem lagomorph branch (F86A, T93N, L116 T) resulted in a pigment identical to that of *Oryctolagus cuniculus* (European rabbit; $\lambda_{max} = 425$ nm [72]), representing a novel mechanism for inducing a shift to a VS pigment. Whether one or a combination of these substitutions causes the shift will need to be verified with mutagenesis studies.

The timetree we used for phylogenetic comparative analyses is in the electronic supplementary material (dataset S4). The SiMMAP results ($n = 163$; table 1) indicate that photic niche is significantly correlated with spectral tuning. For both the unordered and ordered results, scotopic niche is positively associated with a UVS pigment and negatively associated with a VS pigment, whereas photopic niche is negatively associated with a UVS pigment and positively associated with a VS pigment, with one exception (m(Ph,UVS) ordered, $p = 0.08$). Mesopic niche is negatively correlated with UVS pigments and positively with VS pigments, though only when photic niche was ordered. As predicted, the strength of these correlations was generally weaker than those for photopic niche.

The phylogenetic logistic regression analyses (table 2; electronic supplementary material, figures S1 and S2) indicate that increases in both log eye length and log longevity significantly predict UVS to VS pigment shifts. Log eye length has a larger effect on spectral tuning ($\beta = 3.24$) than log longevity ($\beta = 0.908$), suggesting that eye length's association with SWS1 evolution is more important than longevity.

Our PGLS results corroborate the SiMMAP and phylogenetic logistic regression results with one important caveat. Photic niche, log longevity and log eye length all individually have a positive relationship with SWS1 λ_{max} (table 3; electronic supplementary material, figures S3–S5), with log eye length predicting λ_{max} better ($R^2 = 0.3595$) than log longevity ($R^2 = 0.1601$) and photic niche ($R^2 = 0.08559$). However, the results of our multiple regression analyses demonstrate that only log eye length and photic niche contribute to λ_{max} (adjusted $R^2 = 0.4093$). Both eye length and longevity are highly correlated with body size [73,74], which may explain why log longevity's effect on λ_{max} drops out in multiple regression analyses.

Since the term 'mesopic' (cathemeral/crepuscular) covers a broad range of light exposure conditions, it may mask a larger effect of photic niche on λ_{max}. We performed additional PGLS analyses with photic niche recoded as a binary trait by eliminating mesopic species (photic niche B: scotopic = 0, photopic = 1). With this alternative coding, photic niche provides better predictions of λ_{max}, both individually ($R^2 = 0.1571$; table 3; electronic supplementary material, figure S6) and with eye length (adjusted multiple $R^2 = 0.5884$). Photic niche's weaker effect on λ_{max} in the individual PGLS analyses may be an artefact of recoding a continuous character as a discrete character and/or a higher rate of evolution for photic niche than SWS1 spectral tuning. The latter hypothesis is supported by our MCMC analyses in SiMMAP (mean photic niche rate: 0.013; mean spectral tuning rate: 0.00245). Nonetheless, photic niche appears to influence the evolution of ocular lens transmittance, which may in turn drive SWS1 evolution. We performed a PGLS analysis on Douglas & Jeffery's [32] dataset and confirmed that species that occupy brighter niches have lenses that transmit less UV light ($n = 19$; coefficient $= -30.187$; $R^2 = 0.6819$; $p = 1.336 \times 10^{-5}$; Pagel's $\lambda = 0$; electronic supplementary material, figure S7).

Our results suggest that mammalian UVS SWS1 pigments were inherited from an amniote ancestor and maintained in small-eyed species that occupy dim-light niches. The evolution of VS pigments was probably driven in part by increases in light exposure and eye length. We hypothesize that occupying brighter niches and evolving longer eyes decreased transmittance of UV via the ocular media [34], facilitating selection for VS pigments to maximize photon capture. The evolution of lenses with decreased UV transmittance may have been driven by selection pressure(s) to reduce chromatic aberration and/or retinal exposure to harmful UV radiation in bright light. The evolution of longer eyes may be largely a secondary effect of increased body size, since body size positively correlates with eye length. Increases in both light exposure and eye length may ultimately be traced to mammalian niche diversification that occurred after the K–Pg mass extinction. Mammals in the Mesozoic were generally small-bodied and probably nocturnal [75], features

Table 2. Results from phylogenetic logistic regression analyses. Eye length and longevity are log-transformed.

predictor	*n*	β	*p*-value	bootstrap *p*-value
eye length	98	3.2354 ± 0.6896	2.71×10^{-6}	0
longevity	162	0.90765 ± 0.1972	4.17×10^{-6}	0

Table 3. Results from PGLS analyses. Eye length and longevity are log-transformed. The dependent variable in all cases is λ_{max}. Bold *p*-values are <0.05.

predictor	*n*	coefficient	R^2	adjusted R^2	*p*-value
eye length	45	54.465	0.3595		**1.35×10^{-5}**
longevity	54	25.1702	0.1601		**0.00272**
photic niche	50	6.4915	0.08559		**0.0392**
eye length + longevity	42			0.3384	**9.74×10^{-5}**
eye length		53.7523			**0.00171**
longevity		1.8035			0.87901
eye length + photic niche	37			0.4093	**3.77×10^{-5}**
eye length		35.812			**0.00907**
photic niche		15.7822			**0.00145**
longevity + photic niche	46			0.1062	**0.0318**
longevity		14.9755			0.0827
photic niche		5.0101			0.1517
eye length + longevity + photic niche	34			0.4031	**1.99×10^{-4}**
eye length		44.0483			**0.0201**
longevity		−6.012			0.6
photic niche		15.9425			**0.00232**
photic niche B	35	15.7639	0.1571		**0.0184**
eye length + photic niche B	23			0.5884	**3.44×10^{-5}**
eye length		38.6457			**0.0327**
photic niche B		42.7075			**1.83×10^{-4}**
longevity + photic niche B	32			0.08967	0.0928
longevity		8.4025			0.416
photic niche B		12.7197			0.104
eye length + longevity + photic niche B	21			0.5927	**1.46×10^{-4}**
eye length		53.1516			**0.0236**
longevity		−8.8661			0.377
photic niche B		42.6962			**3.04×10^{-4}**

typically attributed to predation by, and/or competition with, dinosaurs. Many mammals evolved larger body sizes after the extinction of non-avian dinosaurs [76] and others may have become more active during the day, resulting in decreased ocular transmittance of ultraviolet light and selection for violet-sensitive SWS1. If the UVS to VS shifts occurred at the midpoint of their respective branches (figure 1), then six of 10 occurred within approximately 10 Myr of the K–Pg boundary. Though a very crude estimate of the timing of these shifts, it implies that this major niche diversification event may have ultimately driven SWS1 evolution.

Data accessibility. New DNA sequences were deposited in GenBank (KT221553–KT221609). Accession numbers for all sequences can be found in the electronic supplementary material, tables S1 and S6. DNA alignments and phylogenies are uploaded as electronic supplementary material (datasets S1–S4).

Authors' contributions. C.A.E. and M.S.S. conceived of and designed the study and wrote the manuscript; C.A.E., H.T.H., M.A.N., R.W.M. and M.S.S. collected the data; C.A.E. and R.W.M. generated *de novo* sequence data; C.A.E. analysed the data. All authors approved the final version of this manuscript.

Competing interests. We declare we have no competing interests.

Funding. This research was funded by NSF grant no. EF0629860 (M.S.S.) and an American Society of Mammalogists Grant-In-Aid of Research (C.A.E.).

Acknowledgements. We thank three anonymous reviewers for comments on an earlier version of this manuscript.

References

1. Jacobs G, Neitz J, Deegan J. 1991 Retinal receptors in rodents maximally sensitive to ultraviolet light. *Nature* **353**, 655–656. (doi:10.1038/353655a0)
2. Calderone JB, Jacobs GH. 1999 Cone receptor variations and their functional consequences in two species of hamster. *Vis. Neurosci*. **16**, 53–63. (doi:10.1017/S0952523899161029)
3. Jacobs GH, Calderone JB, Fenwick JA, Krogh K, Williams GA. 2003 Visual adaptations in a diurnal rodent, *Octodon degus*. *J. Comp. Physiol. A. Neuroethol. Sens. Neural. Behav. Physiol*. **189**, 347–361. (doi:10.1007/s00359-003-0408-0)
4. Williams GA, Calderone JB, Jacobs GH. 2005 Photoreceptors and photopigments in a subterranean rodent, the pocket gopher (*Thomomys bottae*). *J. Comp. Physiol. A Neuroethol. Sensory, Neural, Behav. Physiol*. **191**, 125–134. (doi:10.1007/s00359-004-0578-4)
5. Peichl L, Chavez AE, Ocampo A, Mena W, Bozinovic F, Palacios AG. 2005 Eye and vision in the subterranean rodent cururo (*Spalacopus cyanus*, Octodontidae). *J. Comp. Neurol*. **486**, 197–208. (doi:10.1002/cne.20491)
6. Schleich CE, Vielma A, Glösmann M, Palacios AG, Peichl L. 2010 Retinal photoreceptors of two subterranean tuco-tuco species (Rodentia, *Ctenomys*): morphology, topography, and spectral sensitivity. *J. Comp. Neurol*. **518**, 4001–4015. (doi:10.1002/cne.22440)
7. Arrese CA, Hart NS, Thomas N, Beazley LD, Shand J. 2002 Trichromacy in Australian marsupials. *Curr. Biol*. **12**, 657–660. (doi:10.1016/S0960-9822(02)00772-8)
8. Hunt DM, Chan J, Carvalho LS, Hokoc JN, Ferguson MC, Arrese CA, Beazley LD. 2009 Cone visual pigments in two species of South American marsupials. *Gene* **433**, 50–55. (doi:10.1016/j.gene.2008.12.006)
9. Palacios AG, Bozinovic F, Vielma A, Arrese CA, Hunt DM, Peichl L. 2010 Retinal photoreceptor arrangement, SWS1 and LWS opsin sequence, and electroretinography in the South American marsupial *Thylamys elegans* (Waterhouse, 1839). *J. Comp. Neurol*. **518**, 1589–1602. (doi:10.1002/cne.22292)
10. Gaillard F, Kuny S, Sauvé Y. 2009 Topographic arrangement of S-cone photoreceptors in the retina of the diurnal Nile grass rat (*Arvicanthis niloticus*). *Invest. Ophthalmol. Vis. Sci*. **50**, 5426–5434. (doi:10.1167/iovs.09-3896)
11. Arbogast P, Glösmann M, Peichl L. 2013 Retinal cone photoreceptors of the deer mouse *Peromyscus maniculatus*: development, topography, opsin expression and spectral tuning. *PLoS ONE* **8**, e80910. (doi:10.1371/journal.pone.0080910)
12. Emerling CA, Springer MS. 2014 Eyes underground: Regression of visual protein networks in subterranean mammals. *Mol. Phylogenet. Evol*. **78**, 260–270. (doi:10.1016/j.ympev.2014.05.016)
13. Strachan J, Chang L-YE, Wakefield MJ, Graves JAM, Deeb SS. 2004 Cone visual pigments of the Australian marsupials, the stripe-faced and fat-tailed dunnarts: sequence and inferred spectral properties. *Vis. Neurosci*. **21**, 223–229. (doi:10.1017/S0952523804213281)
14. Arrese CA, Oddy AY, Runham PB, Hart NS, Shand J, Hunt DM, Beazley LD. 2005 Cone topography and spectral sensitivity in two potentially trichromatic marsupials, the quokka (*Setonix brachyurus*) and quenda (*Isoodon obesulus*). *Proc. R. Soc. B* **272**, 791–796. (doi:10.1098/rspb.2004.3009)
15. Deeb SS. 2010 Visual pigments and colour vision in marsupials and monotremes. In *Marsupial genetics and genomics* (eds PD Waters, JE Deakin, JM Graves), pp. 403–414. Dordrecht, The Netherlands: Springer.
16. Wang D, Oakley T, Mower J, Shimmin LC, Yim S, Honeycutt RL, Tsao H, Li W-H. 2004 Molecular evolution of bat color vision genes. *Mol. Biol. Evol*. **21**, 295–302. (doi:10.1093/molbev/msh015)
17. Zhao H, Rossiter SJ, Teeling EC, Li C, Cotton JA, Zhang S. 2009 The evolution of color vision in nocturnal mammals. *Proc. Natl Acad. Sci. USA* **106**, 8980–8985. (doi:10.1073/pnas.0813201106)
18. Müller B, Glösmann M, Peichl L, Knop GC, Hagemann C, Ammermüller J. 2009 Bat eyes have ultraviolet-sensitive cone photoreceptors. *PLoS ONE* **4**, e6390. (doi:10.1371/journal.pone.0006390)
19. Feller KD, Lagerholm S, Clubwala R, Silver MT, Haughey D, Ryan JM, Loew ER, Deutschlander ME, Kenyon KL. 2009 Characterization of photoreceptor cell types in the little brown bat *Myotis lucifugus* (Vespertilionidae). *Comp. Biochem. Physiol. Part B* **154**, 412–418. (doi:10.1016/j.cbpb.2009.08.006)
20. Glösmann M, Steiner M, Ahnelt PK. 2008 Cone photoreceptors and potential UV vision in a subterranean insectivore, the European mole. *J. Vis*. **8**, 1–12. (doi:10.1167/8.4.23.Introduction)
21. Honkavaara J, Koivula M, Korpimaki E, Siitari H, Viitala J. 2002 Ultraviolet vision and foraging in terrestrial vertebrates. *Oikos* **98**, 505–511. (doi:10.1034/j.1600-0706.2002.980315.x)
22. Zhao H, Xu D, Zhou Y, Flanders J, Zhang S. 2009 Evolution of opsin genes reveals a functional role of vision in the echolocating little brown bat (*Myotis lucifugus*). *Biochem. Syst. Ecol*. **37**, 154–161. (doi:10.1016/j.bse.2009.03.001)
23. Melin AD, Moritz GL, Fosbury RAE, Kawamura S, Dominy NJ. 2012 Why aye-ayes see blue. *Am. J. Primatol*. **74**, 185–192. (doi:10.1002/ajp.21996)
24. Jacobs GH. 1992 Ultraviolet vision in vertebrates. *Am. Zool*. **32**, 544–554. (doi:10.1093/icb/32.4.544)
25. Chiao CC, Vorobyev M, Cronin TW, Osorio D. 2000 Spectral tuning of dichromats to natural scenes. *Vision Res*. **40**, 3257–3271. (doi:10.1016/S0042-6989(00)00156-5)
26. Vorobyev M. 2003 Coloured oil droplets enhance colour discrimination. *Proc. R. Soc. Lond. B* **270**, 1255–1261. (doi:10.1098/rspb.2003.2381)
27. Gouras P, Ekesten B. 2004 Why do mice have ultraviolet vision? *Exp. Eye Res*. **79**, 887–892. (doi:10.1016/j.exer.2004.06.031)
28. Hunt DM, Peichl L. 2013 S cones: evolution, retinal distribution, development, and spectral sensitivity. *Vis. Neurosci*. **31**, 115–138. (doi:10.1017/S0952523813000242)
29. Goldsmith TH. 1990 Optimization, constraint, and history in the evolution of eyes. *Q. Rev. Biol*. **65**, 281–322. (doi:10.1086/416840)
30. Cooper GF, Robson JG. 1969 The yellow colour of the lens of man and other primates. *J. Physiol*. **203**, 411–417. (doi:10.1113/jphysiol.1969.sp008871)
31. Hut RA, Scheper A, Daan S. 2000 Can the circadian system of a diurnal and a nocturnal rodent entrain to ultraviolet light? *J. Comp. Physiol. A Sensory, Neural, Behav. Physiol*. **186**, 707–715. (doi:10.1007/s003590000124)
32. Douglas RH, Jeffery G. 2014 The spectral transmission of ocular media suggests ultraviolet sensitivity is widespread among mammals. *Proc. R. Soc. B* **281**, 20132995. (doi:10.1098/rspb.2013.2995)
33. Hart NS. 2001 The visual ecology of avian photoreceptors. *Prog. Retin. Eye Res*. **20**, 675–703. (doi:10.1016/S1350-9462(01)00009-X)
34. Lind O, Mitkus M, Olsson P, Kelber A. 2014 Ultraviolet vision in birds: the importance of transparent eye media. *Proc. R. Soc. B* **281**, 20132209. (doi:10.1098/rspb.2013.2209)
35. Drummond AJ, Ashton B, Buxton S, Cheung M, Cooper A, Duran C, Heled J. 2012 Geneious v. 5.6.5. See http://www.geneious.com.
36. Edgar RC. 2004 Muscle: multiple sequence alignment with high accuracy and high throughput. *Nucleic Acids Res*. **32**, 1792–1797. (doi:10.1093/nar/gkh340)
37. Rambaut A. 1996 Se-Al: Sequence alignment editor. See http://tree.bio.ed.ac.uk/software/seal/.
38. Jones KE *et al.* 2009 PanTHERIA: a species-level database of life history, ecology, and geography of extant and recently extinct mammals. *Ecology* **90**, 2648. (doi:10.1890/08-1494.1)
39. Tacutu R, Craig T, Budovsky A, Wuttke D, Lehmann G, Taranukha D, Costa J, Fraifeld VE, de Magalhães JP. 2013 Human Ageing Genomic Resources: integrated databases and tools for the biology and genetics of ageing. *Nucleic Acids Res*. **41**, D1027–D1033. (doi:10.1093/nar/gks1155)
40. Hall MI, Kamilar JM, Kirk EC. 2012 Eye shape and the nocturnal bottleneck of mammals. *Proc. R. Soc. B* **279**, 4962–4968. (doi:10.1098/rspb.2012.2258)
41. Roll U, Dayan T, Kronfeld-Schor N. 2006 On the role of phylogeny in determining activity patterns of rodents. *Evol. Ecol*. **20**, 479–490. (doi:10.1007/s10682-006-0015-y)
42. Yang Z. 2007 PAML 4: phylogenetic analysis by maximum likelihood. *Mol. Biol. Evol*. **24**, 1586–1591. (doi:10.1093/molbev/msm088)
43. Yokoyama S. 2008 Evolution of dim-light and color vision pigments. *Annu. Rev. Genomics Hum. Genet*. **9**, 259–822. (doi:10.1146/annurev.genom.9.081307.164228)

44. Cowing JA, Poopalasundaram S, Wilkie SE, Robinson PR, Bowmaker JK, Hunt DM. 2002 The molecular mechanism for the spectral shifts between vertebrate ultraviolet- and violet-sensitive cone visual pigments. *Biochem. J.* **367**, 129–135. (doi:10.1042/BJ20020483)
45. Fasick JI, Applebury ML, Oprian DD. 2002 Spectral tuning in the mammalian short-wavelength sensitive cone pigments. *Biochemistry* **41**, 6860–6865. (doi:10.1021/bi0200413)
46. Hunt DM, Cowing JA, Wilkie SE, Parry JWL, Poopalasundaram S, Bowmaker JK. 2004 Divergent mechanisms for the tuning of shortwave sensitive visual pigments in vertebrates. *Photochem. Photobiol. Sci.* **3**, 713–720. (doi:10.1039/b314693f)
47. Parry JWL, Poopalasundaram S, Bowmaker JK, Hunt DM. 2004 A novel amino acid substitution is responsible for spectral tuning in a rodent violet-sensitive visual pigment. *Biochemistry* **43**, 8014–8020. (doi:10.1021/bi049478w)
48. Yokoyama S, Takenaka N, Agnew DW, Shoshani J. 2005 Elephants and human color-blind deuteranopes have identical sets of visual pigments. *Genetics* **170**, 335–344. (doi:10.1534/genetics.104.039511)
49. Carvalho LDS, Cowing JA, Wilkie SE, Bowmaker JK, Hunt DM. 2006 Shortwave visual sensitivity in tree and flying squirrels reflects changes in lifestyle. *Curr. Biol.* **16**, R81–R83. (doi:10.1016/j.cub.2006.01.045)
50. Yokoyama S, Shi Y. 2000 Genetics and evolution of ultraviolet vision in vertebrates. *FEBS Lett.* **486**, 167–172. (doi:10.1016/S0014-5793(00)02269-9)
51. Shi Y, Radlwimmer FB, Yokoyama S. 2001 Molecular genetics and the evolution of ultraviolet vision in vertebrates. *Proc. Natl Acad. Sci. USA* **98**, 11 731–11 736. (doi:10.1073/pnas.201257398)
52. Carvalho LS, Davies WL, Robinson PR, Hunt DM. 2012 Spectral tuning and evolution of primate short-wavelength-sensitive visual pigments. *Proc. R. Soc. B* **279**, 387–393. (doi:10.1098/rspb.2011.0782)
53. Meredith RW *et al.* 2011 Impacts of the Cretaceous Terrestrial Revolution and KPg extinction on mammal diversification. *Science* **334**, 521–524. (doi:10.1126/science.1211028)
54. Meredith RW, Gatesy J, Emerling CA, York VM, Springer MS. 2013 Rod monochromacy and the coevolution of cetacean retinal opsins. *PLoS Genet.* **9**, e1003432. (doi:10.1371/journal.pgen.1003432)
55. Vaidya G, Lohman DJ, Meier R. 2011 SequenceMatrix: Concatenation software for the fast assembly of multi-gene datasets with character set and codon information. *Cladistics* **27**, 171–180. (doi:10.1111/j.1096-0031.2010.00329.x)
56. Stamatakis A. 2014 RAxML version 8: A tool for phylogenetic analysis and post-analysis of large phylogenies. *Bioinformatics* **30**, 1312–1313. (doi:10.1093/bioinformatics/btu033)
57. Miller MA, Pfeiffer W, Schwartz T. 2010 Creating the CIPRES Science Gateway for inference of large phylogenetic trees. In *2010 Gateway Computing Environments Workshop, New Orleans, LA, 14 November 2010*, pp. 45–52. New York, NY: IEEE.
58. Paradis E, Claude J, Strimmer K. 2004 APE: analyses of phylogenetics and evolution in R language. *Bioinformatics* **20**, 289–290. (doi:10.1093/bioinformatics/btg412)
59. Paradis E. 2013 Molecular dating of phylogenies by likelihood methods: a comparison of models and a new information criterion. *Mol. Phylogenet. Evol.* **67**, 436–444. (doi:10.1016/j.ympev.2013.02.008)
60. R Core Team. 2013 *R: a language and environment for statistical computing*. Vienna, Austria: R Foundation for Statistical Computing. See http://www.r-project.org/.
61. Huelsenbeck JP, Nielsen R, Bollback JP. 2003 Stochastic mapping of morphological characters. *Syst. Biol.* **52**, 131–158. (doi:10.1080/10635150390192780)
62. Bollback JP. 2006 SIMMAP: stochastic character mapping of discrete traits on phylogenies. *BMC Bioinform.* **7**, 88. (doi:10.1186/1471-2105-7-88)
63. Schultz TR, Churchill GA. 1999 The role of subjectivity in reconstructing ancestral character states: a Bayesian approach to unknown rates, states, and transformation asymmetries. *Syst. Biol.* **48**, 651–664. (doi:0.1080/106351599260229)
64. Ives AR, Garland T. 2010 Phylogenetic logistic regression for binary dependent variables. *Syst. Biol.* **59**, 9–26. (doi:10.1093/sysbio/syp074)
65. MathWorks. 2015 Matlab version 8.5. See http://www.mathworks.com/products/matlab/.
66. Grafen A. 1989 The phylogenetic regression. *Phil. Trans. R. Soc. Lond. B* **326**, 119–157. (doi:10.1098/rstb.1989.0106)
67. Orme D, Freckleton R, Thomas G, Petzoldt T, Fritz S, Isaac N, Pearse W. 2013 caper: comparative analyses of phylogenetics and evolution in R. See http://cranr-projectorg/web/packages/caper/indexhtml.
68. Sweet G. 1906 Memoirs: contributions to our knowledge of the anatomy of *Notoryctes typhlops*, Stirling. *Q. J. Microsc. Sci.* **2**, 547–572.
69. Peichl L, Behrmann G, Kröger RH. 2001 For whales and seals the ocean is not blue: a visual pigment loss in marine mammals. *Eur. J. Neurosci.* **13**, 1520–1528. (doi:10.1046/j.0953-816x.2001.01533.x)
70. Levenson DH, Ponganis PJ, Crognale MA, Deegan JF, Dizon A, Jacobs GH. 2006 Visual pigments of marine carnivores: pinnipeds, polar bear, and sea otter. *J. Comp. Physiol. A. Neuroethol. Sens. Neural. Behav. Physiol.* **192**, 833–843. (doi:10.1007/s00359-006-0121-x)
71. Emerling CA, Springer MS. 2015 Genomic evidence for rod monochromacy in sloths and armadillos suggests early subterranean history for Xenarthra. *Proc. R. Soc. B* **282**, 20142192. (doi:10.1098/rspb.2014.2192)
72. Nuboer J, Van Nuys W, Wortel J. 1983 Cone systems in the rabbit retina revealed by ERG-null-detection. *J. Comp. Physiol. A* **151**, 347–352. (doi:10.1007/BF00623909)
73. Howland HC, Merola S, Basarab JR. 2004 The allometry and scaling of the size of vertebrate eyes. *Vision Res.* **44**, 2043–2065. (doi:10.1016/j.visres.2004.03.023)
74. Speakman JR. 2005 Body size, energy metabolism and lifespan. *J. Exp. Biol.* **208**, 1717–1730. (doi:10.1242/jeb.01556)
75. Kemp TS. 2005 *The origin and evolution of mammals*. Oxford, UK: Oxford University Press.
76. Smith FA *et al.* 2010 The evolution of maximum body size of terrestrial mammals. *Science* **330**, 1216–1219. (doi:10.1126/science.1194830)